The electronic and magnetic properties of (Mn,C)-codoped ZnO diluted magnetic semiconductor*

Zhao Long(赵 龙), Lu Peng-Fei(芦鹏飞), Yu Zhong-Yuan(俞重远)†,
Ma Shi-Jia(马世甲), Ding Lu(丁 路), and Liu Jian-Tao(刘建涛)

Key Laboratory of Information Photonics and Optical Communications of Ministry of Education, Beijing University of Posts and Telecommunications, Beijing 100876, *China*

(Received 9 January 2012; revised manuscript received 1 March 2012)

The electronic and magnetic properties of (Mn,C)-codoped ZnO are studied in the Perdew–Burke–Ernzerhof form of generalized gradient approximation of the density functional theory. By investigating five geometrical configurations, we find that Mn doped ZnO exhibits anti-ferromagnetic or spin-glass behaviour, and there are no carriers to mediate the long range ferromagnetic (FM) interaction without acceptor co-doping. We observe that the FM interaction for (Mn,C)-codoped ZnO is due to the hybridization between C 2p and Mn 3d states, which is strong enough to lead to hole-mediated ferromagnetism at room temperature. Meanwhile, We demonstrate that ZnO co-doped with Mn and C has a stable FM ground state and show that the (Mn,C)-codoped ZnO is FM semiconductor with super-high Curie temperature ($T_C = 5475$ K). These results are conducive to the design of dilute magnetic semiconductors with codopants for spintronics applications.

Keywords: density functional theory, electronic structure, magnetism, Curie temperature

PACS: 71.15.Mb, 75.50.Pp **DOI:** 10.1088/1674-1056/21/9/097103

1. Introduction

ZnO is a room-temperature semiconductor material with a direct wide band gap of 3.37 eV and a large excitonic binding energy of 60 meV and it has wide prospects in optoelectronic applications. ZnO-based diluted magnetic semiconductors (DMSs) have been actively investigated because it combines the advantages of having logic, memory and communication on a single chip.[1] However, it is still a major challenge nowadays to facilitate ZnO-based DMSs with a high Curie temperature T_C.

In practice, various experimental and theoretical explorations have shown that the 3d transition-metal (TM)-doped bulk or films exhibit magnetic order and the TM atoms prefer to substitute the Zn atoms.[2] Among these TMs, Mn is a ferromagnetic element widely used in doping II–VI-based or III–V-based hosts, such as Mn–ZnO[3−6] and Mn–GaN[7] with higher T_C than room temperature. Luo *et al.*[3] have found that the Mn–Mn interaction is dominated by antiferromagnetic (AFM) coupling from the Curie–Weiss behaviour of susceptibility at high temperature in $Zn_{1-x}Mn_xO$ compounds. In order to raise the Curie temperature and magnetization, one effective method is to codope other metal elements with Mn. Chambers *et al.*[8] have observed that spin-coated N-capped Mn:ZnO nanoparticle films also exhibit room-temperature ferromagnetism by complementary growth method, and suggested that the observed ferromagnetism in Mn:ZnO is mediated by holes. Using the density functional calculations, Zhu *et al.*[9] reported that both Li and Cu tend to segregate into the region near Mn atoms and strongly promote the ferromagnetic (FM) coupling between Mn spins.

Recently, experimental studies indicated the possibility of C doping at the O sites in ZnO.[10,11] In addition, Zhou *et al.*[12] fabricated C-doped ZnO thin films using ion beam technique and found that their Curie temperature is above room temperature. Considering two extended p-type holes brought from carbon in (Mn,C) codoped ZnO, it is worth investigating the carrier-induced ferromagnetism in the ZnO-based DMSs.

The purpose of this paper is to extend the previous simulations, by addressing the electronic struc-

*Project supported by Beijing University of Posts and Telecommunications Excellent Ph. D. Student Foundation, China (Grant No. CX201114), the National Natural Science Foundation of China (Grant No. 61102024), and the Fundamental Research Funds for the Central Universities of China (Grant No. 2012RC0401).

†Corresponding author. E-mail: yuzhongyuan30@gmail.com

© 2012 Chinese Physical Society and IOP Publishing Ltd

ture and magnetic properties of Mn-doped ZnO and (Mn,C)-codoped ZnO. The rest of the present paper is organized as follows. The basic ingredients and the details of our computational method are described in Section 2. Our results are given in Section 3. Finally, the conclusions drawn from the present study are given in Section 4.

2. Method

Our simulations are implemented with a plane-wave pseudopotential method based density functional theory (DFT) code,[13] namely the Cambridge serial total energy package (CASTEP) code. The generalized gradient approximation (GGA) in the scheme of Perdew–Burke–Ernzerhof (PBE) is used to treat the exchange-correlation function.[14] Moreover, the valence-electron configurations for the carbon, oxygen, zinc and manganese atoms are employed as $2s^2\ 2p^2$, $2s^2\ 2p^4$, $3d^{10}\ 4s^2$ and $3d^5\ 4s^2$, respectively. The plane-wave functions of valence electrons are expanded in a plane-wave basis set. Reciprocal-space integration over the first Brillouin zone is approximated through a careful sampling at a finite number of k points using a Monkhorst–Pack mesh.[15] The 2×2×2 ZnO supercell containing 32 atoms is used and the supercell is kept at constant volume.

The substitutional method is adopted. For x = 6.25%, only one Zn atom is substituted by Mn, while one O atom is substituted by C for y = 6.25% We perform the geometry optimization of ZnO and the cutoff energy ($E_{\rm cut}$) is set to be 460 eV according to our previous paper.[6] Meanwhile, the k-point set with parameters of 7×7×4 and 4×4×2 for pure ZnO and the $Zn_{1-x}Mn_xO_{1-y}C_y$ alloy, respectively, are used over the first Brillouin zone sampling mesh. Self-consistency is considered to be achieved when the difference of charge densities between succeeding iterations is less than 2×10^{-6} eV per atom. In the optimization process, the energy change, maximum force, maximum stress, and maximum displacement tolerances are set to be 2×10^{-5} eV per atom, 0.05 eV/Å, 0.1 GPa, and 0.002 Å, respectively. In addition, both lattice constants and atomic positions are relaxed whenever available.

3. Results and discussion

3.1. The optimization of the structure $Zn_{1-x}Mn_xO_{1-y}C_y$

A systematic study on the structural geometry optimization of the intrinsic and doped ZnO is investigated. At ambient temperature and pressure, the stable phase of ZnO is of hexagonal wurtzite structure with $P6_3mc$ space group and C_{6v}^4 symmetry. Lattice constants $a = b = 3.249$ Å, $c = 5.202$ Å, and $c/a = 1.601$. All calculations are based on the 2×2×2 supercell model as shown in Fig. 1. The ligand of ZnO is a triangular cone, and the Zn–O bond length along c-axis (1.952 Å) is shorter than that in other directions (1.986 Å). As depicted in Table 1, after optimization, the lattice constants are increased by 0.90% in a and b, and 2.22% in c with respect to experimental lattice constants,[3] but the shape of the hexagonal structure is preserved. To investigate the influence of dopants on the wurtzite structure of host ZnO, a Mn atom substitutes Zn atom on site 17 in Fig. 1. The hexagonal structure is still kept unchanged. The Zn site is substituted by Mn perfectly and the difference between a and b is 0.001 Å, which are in good agreement with previous experimental observations of the structure of bulk ZnO:Mn.[2] For 6.25% concentration of Mn doping, the augment of lattice constants is 0.43% for a and b and 0.12% for c, resulting from the fact that high-spin ionic radius of Mn^{2+} 0.75 Å is larger than the Zn^{2+} 0.60 Å in tetrahedral coordination. Moreover, a similar simulation is repeated by replacing an O atom on site 9 in Fig. 1 with a C atom. Its optimized structure still reflects the conservation of hexagonal structure.

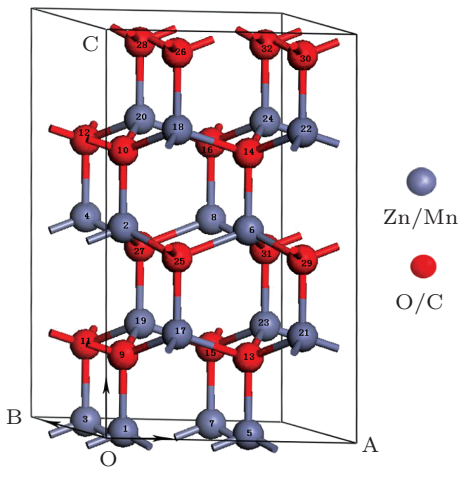


Fig. 1. (colour online) A 32-atom 2×2×2 ZnO supercell with lattice sites labeled.

Table 1. Relaxed structures of $Zn_{16}O_{16}$, $Zn_{15}Mn_1O_{16}$ (Mn substitution of Zn on site 17 in Fig. 1), and $Zn_{16}O_{15}C_1$ (C substitution of O on site 9 in Fig. 1) compared with the experimental structure of $Zn_{16}O_{16}$. The lattice constants (a, b, c), lattice angles (α, β, γ), and the fractional coordinates of lattice sites 17 and 9 are shown.

	a/Å	b/Å	c/Å	α	β	γ	X_9	Y_9	Z_9	X_{17}	Y_{17}	Z_{17}
expt. [3] $Zn_{16}O_{16}$	6.4980	6.4980	10.4040	–	–	–	–	–	–	–	–	–
relaxed $Zn_{16}O_{16}$	6.5579	6.5579	10.6357	90°	90°	120°	0.1667	0.3333	0.1913	0.3333	0.1667	0.2500
relaxed $Zn_{15}Mn_1O_{16}$	6.5861	6.5860	10.6484	90°00′10″	89°59′49″	120°4′13″	–	–	–	0.3334	0.1667	0.2498
relaxed $Zn_{16}O_{15}C_1$	6.5587	6.5584	10.6486	89°59′09″	90°00′50″	120°2′12″	0.1667	0.3333	0.1877	–	–	–

3.2. FM and AFM properties of Mn-doped ZnO

Substitution of two Zn atoms by Mn gives a dopant concentration of 12.5%, which allows for the calculation of the relative energies of FM and AFM orderings. In Fig. 1, there are five different possible sets of substitutional sites: (17,19), (6,17), (8,17), (17,18), and (17,24). We mark these five configurations as I, II, III, IV and V. As listed in Table 2, the ground state is found to be the AFM state of configuration I, 194 meV lower than its FM state in energy. For each Mn–Mn separation, the energy difference between FM and AFM orderings, $\Delta E = (E_{\rm AFM} - E_{\rm FM})/2$, is used as an indicator of the magnetic stability. This quantity determines the stabilization of the magnetic phases in the DMS. The $\Delta E > 0$ corresponds to the fact that the FM phase is more stable than the spin glass phase, and *vice versa*. Thus, the spin-glass state is predicted by calculating the total energy difference ΔE. Moreover, Mn ions prefer to be substituted within the *ab* plane and tend to form clusters. As shown in Table 2, in the Mn–Mn distance range of 3.29–4.65 Å, the total energy differences between the FM and AFM states rapidly decrease; while in the Mn–Mn distance range of 4.65–6.27 Å, ΔE remains constant. Thus, the magnetic coupling between the Mn ions is likely to be short ranged.

Figure 2 shows that the $Zn_{0.875}Mn_{0.125}O$ system possesses no FM behaviour because the AFM state is more stable than the FM state for all configurations. Our simulation is in good agreement with the available experimental results.[5] It can be observed that as Mn ions change from being paired to being isolated, ΔE increases sharply and approaches zero.

Table 2. Total energies of the FM and AFM phases in different configurations for the $Zn_{0.875}Mn_{0.125}O$ supercell. The highest FM energy in configuration I is set to be zero. M means the average unpaired electron number of each Mn atom.

Configuration No.	Position of Mn	Mn–Mn distance/Å	$E_{\rm FM}$/meV	$E_{\rm AFM}$/meV	$M_{\rm FM}/\mu_{\rm B}$	$M_{\rm AFM}/\mu_{\rm B}$	
						$M1$	$M2$
I	17,19	3.299	0	–194.268	4.68	4.70	–4.70
II	6,17	3.334	–21.014	–101.747	4.70	4.72	–4.70
III	8,17	4.657	–42.142	–43.243	4.74	4.74	–4.74
IV	17,18	5.342	–45.089	–48.459	4.74	4.74	–4.74
V	17,24	6.279	–30.948	–31.671	4.74	4.74	–4.74

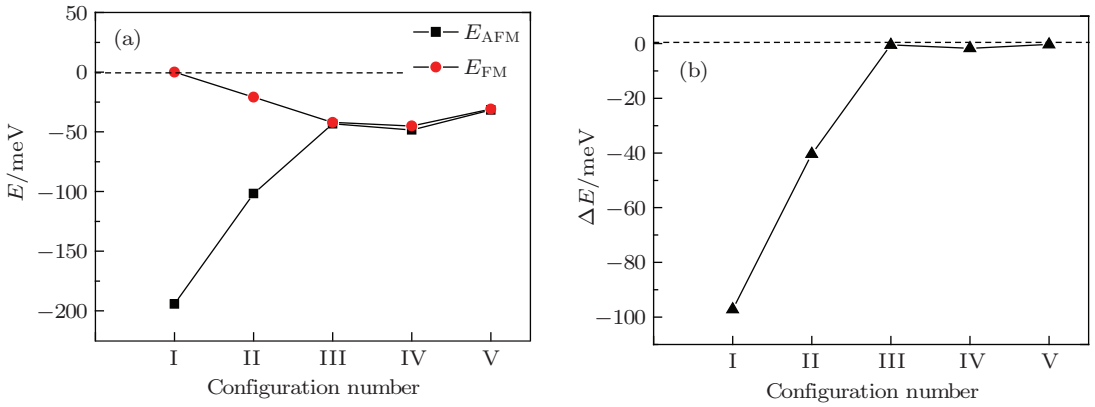


Fig. 2. (colour online) (a) Total energy per supercell for AFM ($E_{\rm AFM}$)and FM ($E_{\rm FM}$) states and (b) the difference in total energy per Mn between AFM and FM (ΔE) for different geometry configurations. $E_{\rm FM}$ with highest total energy was chosen as an energy reference in configuration I for $Zn_{14}Mn_2O_{16}$ alloy.

3.3. FM and AFM properties of (Mn,C)-codoped ZnO

For $Zn_{14}Mn_2O_{15}C_1$ alloy, one Mn atom and one C atom are fixed at the positions of 17 and 25, respectively. The other Mn atom moves at the different positions to form configurations 1–5, which is shown in Table 3. According to our calculations, $E^5_{\rm AFM}$ with highest total energy is chosen as an energy reference. A strong tendency toward forming complexes can be clearly observed in Fig. 3. In Configuration 1, when two Mn ions are paired via one C ion along the c direction, a strong FM electronic ground state of $\Delta E^1 = 657$ meV is observed. In Configurations 2–5, when two Mn ions are separated by –O–Zn–C– or –O–Zn–C–Zn–O, the total energies are kept in a higher energy region of −200–0 meV in either AFM or FM. It indicates that by codoping with C atom, the magnetic properties of ZnMnO system can change from AFM to FM. However, the high $T_{\rm C}$ is dependent on the distance between Mn ions. In addition, for the majority of complexes formed, the electronic ground state is of FM.

Table 3. Total energies of the FM and AFM phases for five geometrically possible configurations of a $Zn_{14}Mn_2O_{15}C_1$ supercell consisting of two Mn atoms and one C atom in a 2×2×2 ZnO supercell with substituent Mn and C sites labeled.

Configuration No.	Position of C	Position of Mn	$E_{\rm FM}$/meV	$E_{\rm AFM}$/meV
1	25	6,17	–676.508	–19.628
2	25	17,19	–40.271	–168.241
3	25	8,17	–34.739	–19.704
4	25	17,18	–34.454	–17.951
5	25	17,24	–27.908	0

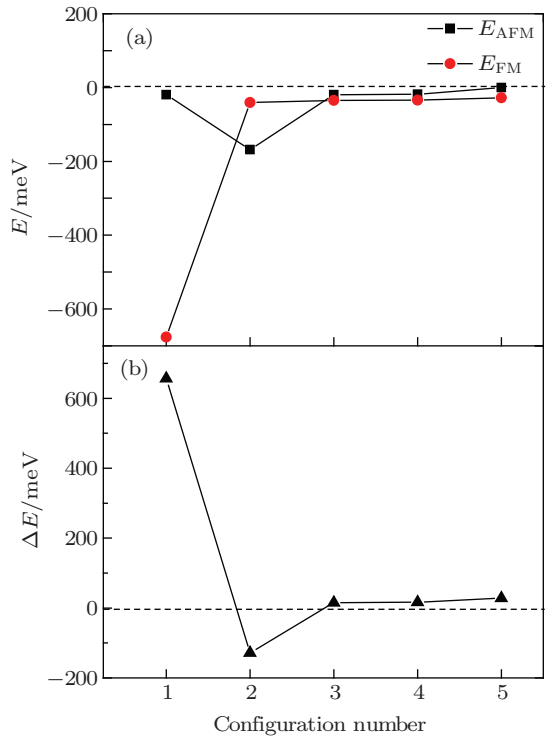


Fig. 3. (colour online) (a) Total energies per supercell for AFM ($E_{\rm AFM}$) and FM ($E_{\rm FM}$) states and (b) the difference in total energy per Mn between AFM and FM (ΔE) for different geometry configurations. $E_{\rm AFM}$ with highest total energy is chosen as an energy reference in configuration 5 for $Zn_{14}Mn_2O_{15}C_1$ alloy.

Up to now, the optimal way to estimate $T_{\rm C}$ is still an interesting and challenging topic. The $T_{\rm C}$ of DMS material is estimated by calculating p–d exchange interactions[16,17] and using the mean-field approximation.[18] These previous calculations seem always to overestimate $T_{\rm C}$ compared with exact calculation by Monte Carlo (MC) method. MC method requires large cost of computation that is computationally impossible in principle, so the classical Heisenberg model is used to treat the energy difference between the AFM state and the FM state as discussed in Ref. [19], where the spin interaction energy in a supercell, Ω, can be expressed as

$$E = -\frac{1}{2}\sum_{j\alpha\neq i}\sum_{i\in\Omega} J(r_{i,j_\alpha}) S_i \cdot S_{j_\alpha}, \qquad (1)$$

where α represents all the supercells expanded in the solid, and S_i and S_j denote the localized magnetic moments. Since the interaction is shared by two atoms, the factor 1/2 is utilized. The $J(r)$ denotes the effective exchange interaction between a pair of magnetic atoms, and provides a suitable tool to describe magnetic properties at finite temperatures. Moreover, we employ mean-field approximation (MFA), which can be written as[18]

$$K_{\rm B}T_{\rm C} = 2\Delta E/3x. \qquad (2)$$

It can be obtained that $T_{\rm C}$ is proportional to ΔE. In previous experiment,[20] a relatively high $T_{\rm C}$ of 350 K was observed for Cu-doped ZnO. In addition, Ye *et al.*[11] performed a similar simulation to obtain a result ($\Delta E = 42$ meV). Thus, our result ($\Delta E^1 = 657$ meV) is large enough to lead to room

temperature ferromagnetism and $T_C^1 = 5475$ K. As depicted in Fig. 3, it is worth noting that although the FM coupling weakly depends on the direction of aligned Mn ions, it largely relies on the distance between two Mn ions. The most stable complexes were found in the configurations where two Mn ions are paired via one C ion, that is, –O–Mn–C–Mn–O–. Our results reveal that the FM state can only be realized at some configurations. However, dopants tend to form complexes rather than stay isolated. Because of the solubility limit of donor impurities, this requirement may be difficult to fulfill. This is probably the reason why it is difficult to obtain FM DMS.

Figure 4 shows the spin distribution for the most stable configuration I (Table 1) and 1(Table 3). In Fig. 4(a), when two Mn ions are paired via one O ion,

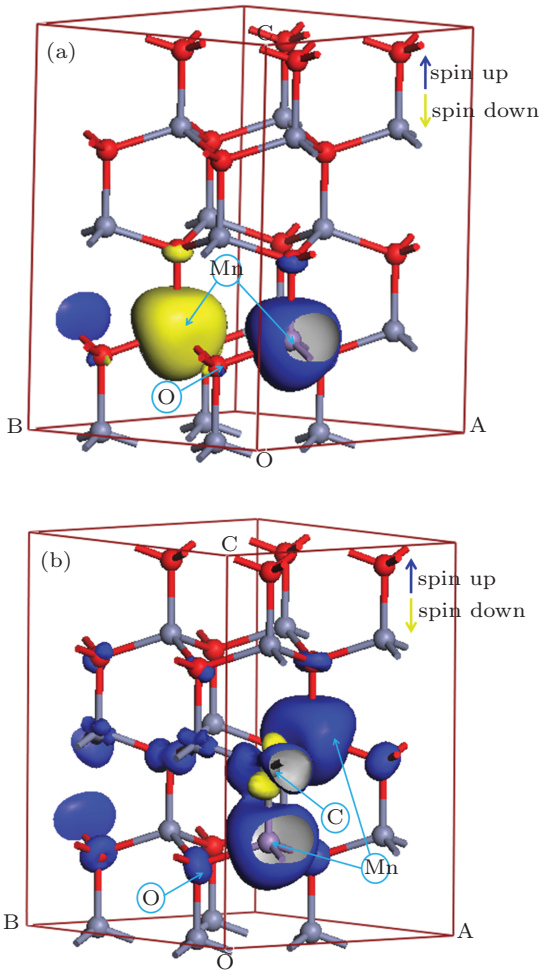


Fig. 4. (colour online) The 3D iso-surface of the spin density for (a) $Zn_{14}Mn_2O_{16}$ in configuration I (AFM state) and (b) $Zn_{14}Mn_2O_{15}C_1$ in configuration 1 (FM state). Iso-surfaces cover all points of the charge density of 0.0263 $e/Å^3$.

each Mn ion magnetizes only four neighbouring oxygen ions. Moreover, it can indicate that when two Mn ions are separated by more than one O ion, no long-range indirect exchange interaction exists among Mn ions. Figure 4(b) shows a three-dimensional (3D) isosurface with an average spin charge density of 0.0263 $e/Å^3$. It is clearly observed that Mn and C ions contribute to the magnetic properties of $Zn_{14}Mn_2O_{15}C_1$ alloy, that is, the unpaired Mn 3d electrons and the unpaired 2p electrons on the neighbouring C ion are responsible for the spin polarization. Comparing Fig. 4(b) with Fig. 4(a), we believe that the distribution of C 2p electrons are wider in range than O 2p electrons.

To gain an insight into the origin of ferromagnetism, electronic structures of configuration I (Table 1) and 1 (Table 3) are investigated. The densities of states (DOSs) in the close configuration for the Mn-doped ZnO and the (Mn, C)-codoped ZnO are illustrated in Fig. 5. For the Mn-doped ZnO, it is interesting to note that despite the hybridization between the Mn 3d and O 2p states, Mn 3d states are rarely distributed around Fermi level and there are no free carriers to mediate the long range FM interaction. Therefore, the super-exchange interaction between the neighbouring Mn^{2+} ions is AFM in character. However, when C atom replaces some of the O sites in the Mn-doped ZnO, the total energy calculations indicate that the Mn and C atoms prefer to exist as the nearest neighbours, which is sketched in Fig. 3. The partial DOSs of Mn 3d and C 2p states of configuration 1 with an AFM state in Fig. 5(b) reveal that they are distributed fairly equally between up-spin and down-spin regions. Comparing Fig. 5(c) with Fig. 5(a), we can clearly see that C ion brings in holes with 0–1.3 eV and the hole state is delocalized. Meanwhile, as can be seen in Fig. 5(c), The DOS peaks around the Fermi energy from Mn 3d and C 2p states indicate their large contributions to the defect bands, which shows that they are heavily mixed. Clearly, the difference between the majority and the minority of spins are due mainly to hybridization of Mn 3d and C 2p states, which leads to the half-metallic character of the $Zn_{0.875}Mn_{0.125}O_{0.9375}C_{0.0625}$ system and hence the holes are 100% spin polarized. Those indicate that ferromagnetism is mediated through the p–d exchange interaction between Mn ions and holes induced by C doping. Our results are in agreement with other theoretical results,[21,22] showing that additional hole carrier is one of the possible mechanisms. Meanwhile, it must be pointed out that the discrepancy can be attributed also to the difference in sample growing condition or sample growing method. Therefore, further work is needed to investigate the magnetic properties

of (Mn,C)-codoped ZnO within the framework of DFT methods.

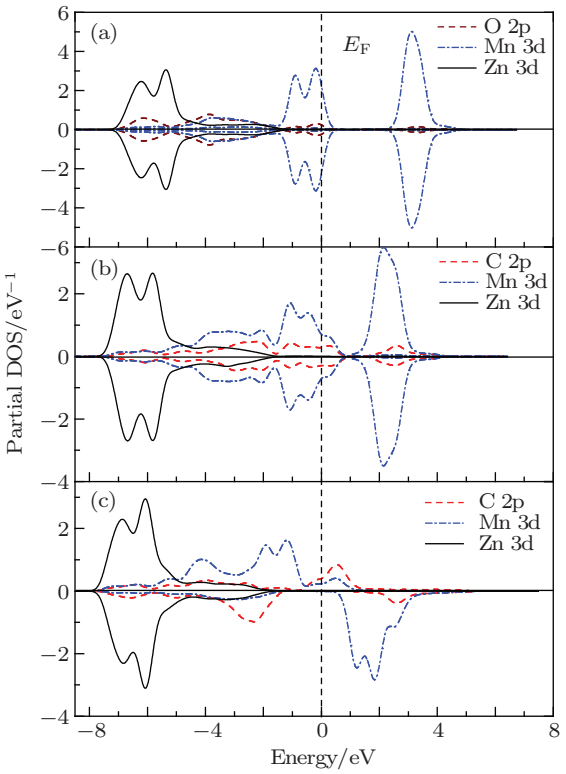


Fig. 5. (colour online) Partial DOS of (a) $Zn_{0.875}Mn_{0.125}O$ in configuration I with an AFM state, and $Zn_{0.875}Mn_{0.125}O_{0.9375}C_{0.0625}$ in configurations 1 with (b) an AFM state and (c) a FM state.

4. Conclusion

In the present paper, a first-principles study is performed to evaluate the electronic and magnetic properties of the $Zn_{1-x}Mn_xO_{1-y}C_y$ system. By investigating 5 geometrical configurations, we demonstrate that Mn doped ZnO exhibits AFM or spin-glass behaviour. Without acceptor co-doping, there are no carriers to mediate the long range FM interaction. We succeed in observing that for (Mn,C)-codoped ZnO, the FM interaction is due to the hybridization between C 2p and Mn 3d states, which is strong enough to lead to hole-mediated ferromagnetism at room temperature. Furthermore, we show that the (Mn,C)-codoped ZnO is FM semiconductor with super-high Curie temperature (T_C = 5475 K). These results are conducive to the design of dilute magnetic semiconductors with codopants for spintronics applications.

Acknowledgment

The authors would like to express their great thanks to the Key Laboratory of Information Photonics and Optical Communications from Beijing University of Posts and Telecommunications for the support of computing facilities.

References

[1] Awschalom D D, Flatte M E and Samarth N 2002 *Sci. Am. Inc.* **286** 67
[2] Gopal P and Spaldin N A 2006 *Phys. Rev.* B **74** 094418
[3] Luo J, Liang J K, Liu Q L, Liu F S, Zhang Y, Sun B J and Rao G H 2005 *J. Appl. Phys.* **97** 086106
[4] Li P, Deng S H, Zhang L, Yu J Y and Liu G H 2010 *Chin. Phys.* B **19** 117102
[5] Cheng X M and Chien C L 2003 *J. Appl. Phys.* **93** 7876
[6] Zhao L, Lu P F, Yu Z Y, Guo X Y, Shen T, Ye H, Yuan G F and Zhang L 2010 *J. Appl. Phys.* **108** 113924
[7] Dietl T, Ohno H, Matsukura F, Cibert J and Ferrand D 2000 *Science* **287** 1019
[8] Chambers S A, Schwartz D A, Liu W K, Kittilstved K R and Gamelin D R 2007 *Appl. Phys.* A **88** 1
[9] Zhu Y, Cao J X, Yang Z Q and Wu R Q 2009 *Phys. Rev.* B **79** 085206
[10] Pan H, Yi J B, Shen L, Wu R Q, Yeng J H, Lin J Y, Feng Y P, Ding J, Van L H and Yin J H 2007 *Phys. Rev. Lett.* **99** 127201
[11] Ye X J, Song H A, Zhong W, Xu M H, Qi X S, Jin C Q, Yang Z X, Au C T and Du Y W 2008 *J. Phys.* D: *Appl. Phys.* **41** 155005
[12] Zhou S, Xu Q, Potzger K, Talut G, Grötzschel R, Fassbender J, Vinnichenko M, Grenzer J, Helm M, Hochmuth H, Lorenz M, Grundmann M and Schmidt H 2008 *Appl. Phys. Lett.* **93** 232507
[13] Perdew J P, Burke K and Ernzerhof M 1996 *Phys. Rev. Lett.* **77** 3865
[14] Payne M C, Teter M P, Allan D C, Arias T A and Joannopoulos J D 1992 *Rev. Mod. Phys.* **64** 1045
[15] Monkhorst H J and Pack J D 1976 *Phys. Rev.* B **13** 5188
[16] Bergqvist L, Eriksson O, Kudrnovsky J, Drchal V, Korzhavyi P and Turek I 2004 *Phys. Rev. Lett.* **93** 137202
[17] Sato K, Schweika W, Dederichs P H and Yoshida H K 2004 *Phys. Rev.* B **70** 201202
[18] Sato K, Dederichs P H and Katayama Y H 2003 *Europhys. Lett.* **61** 403
[19] Zhao Y J, Shishidou T and Freeman A J 2003 *Phys. Rev. Lett.* **90** 047204
[20] Xu H Y, Liu Y C, Xu C S, Liu Y X, Shao C L and Mu R 2006 *Appl. Phys. Lett.* **88** 242502
[21] Lin X L, Yan S S, Zhao M W, Hu S J, Yao X X, Han C, Chen Y X, Liu G L, Dai Y Y and Mei L M 2010 *J. Appl. Phys.* **107** 033903
[22] Shim W Y, Jeon K A, Lee K I, Lee S Y, Jung M H and Lee W Y 2006 *J. Electron. Mater.* **35** 635